# Microfluidic device for delivery of multiple inks for dip pen nanolithography

**Juan Alberto Rivas-Cardona**
**Debjyoti Banerjee**
Texas A&M University
Department of Mechanical Engineering
3123 TAMU
College Station, Texas 77843-3123
E-mail: dbanerjee@tamu.edu

**Abstract.** In the dip pen nanolithography (DPN) process, ultra-sharp scanning probe tips ("pens") are coated with chemical compounds (or "ink") and contacted with a surface to produce submicron-sized features. This work describes the design, fabrication, and testing of a microfluidic ink delivery device for delivering multiple species of inks to an array of multiple pens, as well as for maximizing the number of inks for simultaneous patterning by DPN. The microfluidic device (called "*Centiwell*") consists of a 2-D array of 96 microwells that are obtained by silicon bulk micromachining process. A thermoelectric module is attached to the bottom of the substrate. Microbeads of a hygroscopic material (e.g., polyethylene glycol or PEG) are dispensed into the microwells. The thermoelectric module cools the substrate to below the dew point for condensing water droplets on the microbeads and to create PEG solutions that serve as the ink for DPN. An array of pens is then coated with the ink. Subsequently, nanolithography is performed with the coated pens. Multiple PEG nanopatterns obtained by this method are presented as proof-of-concept. This demonstrates the functionality of the *Centiwell* microfluidic ink delivery device for nanolithography of multiple inks. Also, fractal nanopatterns are observed in the nanolithography experiments.
 [DOI: 10.1117/1.2778685]

Subject terms: thermoelectric; hygroscopic; microbeads; nanofabrication; fractal.

Paper 06061R received Sep. 27, 2006; revised manuscript received Feb. 15, 2007; accepted for publication Apr. 9, 2007; published online Sep. 17, 2007. This paper is a revision of a paper presented at the SPIE conference on Micro (MEMS) and Nanotechnologies for Space Applications. Apr. 2006, Orlando, Florida. The paper presented there appears (unrefereed) in SPIE Proceedings Vol. 6223.

## 1 Introduction

Dip pen nanolithography (DPN) is a versatile nanofabrication platform that leverages microfluidic "ink" delivery systems with scanning probe microscopy and has applications in biotechnology, photomask repair, molecular electronics, nanoelectronics, cryptography (brand protection, encryption, etc.), combinatorial materials discovery, nanocatalysis, and maskless lithography.[1] This novel technique offers a high resolution and multiplexed registration with parallel direct-write printing capabilities. These capabilities make DPN a particularly attractive tool for patterning biological and soft organic structures onto surfaces.

Several research groups have worked on advancing the state-of-the-art of DPN by the development of microelectromechanical systems (MEMS) based parallel-probe arrays for DPN applications,[2–4] as well as prototypes of individually controlled probe arrays[5–8] and passive probe arrays.[9] DPN can be used to fabricate bioarrays with different feature sizes and variety of biochemical species. This is a challenging task that requires ultimately the automated implementation of parallel-pen and integrated-inking systems. Microfluidic devices, customized for specific applications, can solve this challenge by controlling the inking of individual cantilevers in a parallel probe array.

Array-based technologies are used extensively in genomics and proteomics. The contemporary laboratory protocols involve commercial robotic spotting systems with only 4 to 16 pins, which are used to generate custom biochips. Photolithographic processes are used for fabricating bioarrays with feature sizes $\sim 50\ \mu$m.[10] DPN technology (and the microfluidic device described in the present work) can shrink the bioarrays to a spot size of 150 nm or less. The DPN technology can therefore maximize the biological information content in a single chip to match the same information contained in more than 10,000 conventional chips spotted with current technologies.[1] DPN typically requires fluid dispensing volume of 100 pL or less, which is 10,000 times smaller than the capability of commercial robotic dispensers.

Hence, a need exists for maximizing the number of chemical species (or "inks") that can be simultaneously delivered in very small volumes ($\sim$100 pL or less) and that can be simultaneously patterned by DPN. This would harness the power of the DPN to meet the industrial standards. For example, the industrial biotechnology standards for bioassays require parallel delivery of 48, 96, 384, or higher numbers of biochemical species. Hence a microfluidics device capable of 96 inks is required for the feasibility of DPN for biotechnology applications. Such a microfluidic device would enable the delivery of 96 or more numbers of inks to an array of open microwells, into which a parallel array of scanning probe tips (or "pens") can be inserted for coating the individual pens with unique chemical species.

1537-1646/2007/$25.00 © 2007 SPIE

Such a delivery device should be capable of preventing any cross contamination between the delivered inks.

Recently, Banerjee et al.[11–13] developed a commercial microfluidic device called "Inkwells™." Inkwells™ deliver multiple inks to an array of pens for subsequent DPN operation. Inkwells™ were designed for biotechnology applications.[14,15] However, the Inkwells platform is limited to the handling of only ten inks for DPN.[16]

The *Centiwell* microfluidic ink delivery device reported in this study maximizes the ink handling capacity for DPN to 96 inks and in a format similar to a microtiter plate. The design, fabrication, assembly, and testing of the *Centiwell* microfluidic device is described in this work.

## 2 Microfabrication of the *Centiwell* Microfluidic Device

The *Centiwell* device consists of an array of microwells fabricated by a combination of bulk micromachining processes. The microwells are squares of 40 $\mu$m on each side, located in an array of 8 by 12, with a center-to-center pitch of 80 $\mu$m to correspond with the pitch of a DPN Multi-Probe Array™ (parallel DPN pens commercially available from Nanoink, Incorporated, Skokie, IL). Unlike the Inkwells™ (where the depth of the microwells was in excess of 100 $\mu$m[15]), the depth of the microwells in this design was ~5 $\mu$m, resulting in microwell volumes of about 1 pL. The microwells were integrated with commercially available thermoelectric modules (or Peltier coolers) by adhesive bonding. As a proof-of-concept, microbeads of polyethylene glycol (PEG) (a hygroscopic material) were dispensed into the microwells to form a bead array colocated with the microwell array. By reducing the temperature of the substrate to below the dew point, water droplets were condensed on the PEG microbeads contained in the microwells. The hygroscopic property of PEG was used to capture the condensed water droplets and to prevent (or minimize) their evaporation from the microwells. This was used to dissolve the beads and to create PEG solutions, which served subsequently as an "ink" for the DPN process.

Figure 1 shows a schematic of the microfluidic ink delivery device with an integrated thermoelectric module. This figure shows only part of the complete array of microwells for better visualization. The complete design of *Centiwell* consists of: 1. the 96-microwell array on a silicon substrate, 2. the thermoelectric module that is attached to the back side of the silicon substrate, and 3. PEG microbeads that are positioned in each microwell. Each PEG microbead positioned in the microwells could be synthesized to contain unique biochemical species (e.g., proteins, peptides, nucleic acid oligomers, etc.) that are subsequently available as inks in PEG solution for DPN.

### 2.1 *Microfabrication of Microwells for the Centiwell Device*

The substrate used for the fabrication of the *Centiwell* device was a ⟨100⟩ silicon wafer three inches in diameter. The microwells were patterned by photolithography and subsequently they were micromachined using a wet etching process. The photomask used for the photolithographic process was designed using AutoCad software and manufactured at the mask-fabrication facility in the Health Science Center at Texas A&M University. The photomask consists of an $8\times12$ array of square patterns of 20 $\mu$m in length and a center-to-center pitch of 80 $\mu$m.

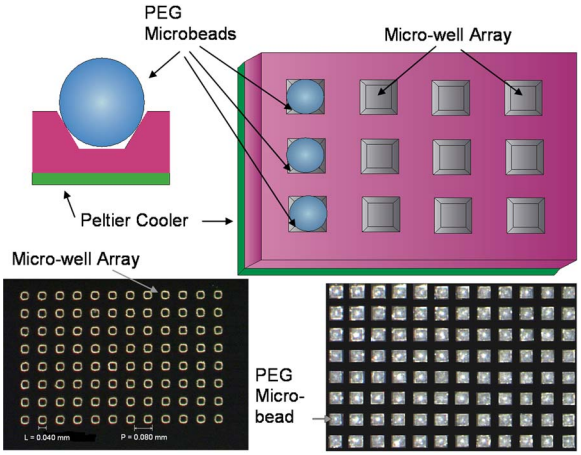


**Fig. 1** Schematic representation of the *Centiwell* microfluidic ink delivery device. There are 96 microwells in an $8\times12$ format, which are designed to be 40 $\mu$m on a side, 5 $\mu$m deep, and on an 80-$\mu$m pitch. This figure shows only part of the complete array of microwells for better visualization. The PEG microbeads were selected to be of a similar size distribution as the microwells. The inset at the bottom shows a picture of the Centiwell using bulk micromachining techniques.

The microwell array of the *Centiwell* microfluidic device was fabricated in a Class 1000 Cleanroom at the Materials Characterization Facility of Texas A&M University. The steps for the microwell fabrication are shown schematically in Fig. 2. These steps include the patterning of photoresist

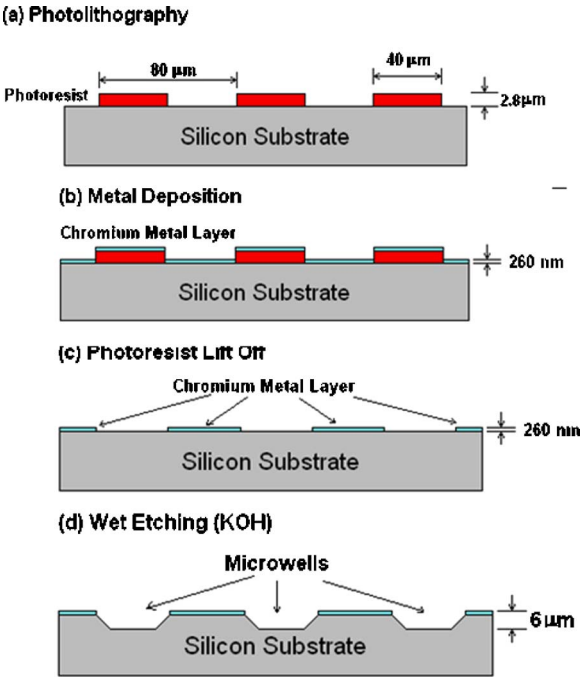


**Fig. 2** Schematic of the microwell fabrication process on silicon substrate.

using photolithography, physical vapor deposition, and patterning of a chromium etch mask by the lift-off process (to serve as a barrier for the etching process), and wet etching of the microwells.

The silicon wafer was initially cleaned in an ultrasonic bath with acetone for 15 min, then rinsed with isopropyl alcohol, and dried with nitrogen gas. A dehydration process was performed by baking the silicon wafer for 5 min at 200°C to vaporize any remaining solvents or contaminants. To improve the adhesion of the photoresist, the silicon wafer was spin-coated with hexamethyldisilazane (HMDS) for 30 s at 3000 rpm, followed by a two-minute soft-bake process at 115°C. Subsequently, Shipley 1827 positive photoresist was spin-coated on the surface of the wafer for 60 s at 3000 rpm, followed by a one-minute soft-bake process at 100°C. The spin-coating process was performed on a SCS P6204 (8-in. bowl) nonprogrammable spin coater. A Quintel Q4000 mask aligner was used to transfer the pattern from the photomask to the photoresist spin-coated on the silicon wafer. Using the mask aligner, the wafer was exposed to a high intensity UV light (wavelength 365 nm) for 45 s. Subsequently, the wafer was immersed in MF-319 developer (by MicroChem, Newton, MA) for 60 s and rinsed with deionized (DI) water. Finally, the patterned wafer was hard-baked for 5 min at 115°C [Fig. 2(a)]. The thickness of the resist layer obtained after photolithography was measured to be 2.8 $\mu$m, using a Dektak 3 Stylus Profilometer (Manufactured by Veeco Instruments, Santa Barbara, CA).

The next step in the fabrication of the microwells for the *Centiwell* was the deposition of a chromium metal layer used as a barrier for the wet etching process [Fig. 2(b)]. To promote the better adherence of the metal layer to the silicon substrate, an oxygen plasma cleaning (de-scum) was performed using March Plasma Systems Model CS-1701 reactive ion etcher (RIE). Although the de-scum process reduces the thickness of the photoresist layer, it helps to remove traces of photoresist in the exposed region of the wafer, improving the yield for the lift-off process.

The chromium layer was vapor-deposited (using a BOC Edwards Auto 306 Metal Evaporation Chamber, BOC Group Incorporated) on the surface of the patterned wafer. The thickness of the chromium layer was approximately 260 nm. The back side of the wafers was also protected with a 700-nm chromium layer. Once the chromium mask was deposited, the photoresist was lifted off using Nano-Strip solution (Rockwood Electronic Materials, Cyantek, Fremont, California). The lift-off process was performed for 6 h in an ultrasonic bath at 50°C [Fig. 2(c)]. At this point, the actual depth of the microwells was found to be 1.5 $\mu$m (measured with Dektak 3 Stylus Profilometer).

Finally, the silicon wafer was immersed in a potassium hydroxide (KOH) solution (30% KOH by weight in water) for 80 min at 80°C [Fig. 2(d)]. Data on etch rates at different KOH concentrations and temperatures, as well as etch-stop mechanisms, have been documented by Seidel et al.,[17,18] and the important results have been summarized by Williams, Gupta, and Wasilik.[19] However, it was observed in the current fabrication that the etch rate was about ten times slower than the one reported in the literature. The depth of the etched microwells was measured with a Dektak 3 Stylus Profilometer and was found to be about 5.8 $\mu$m. The resulting microwells therefore have volumes of ~1 pL. Figure 1 (inset) shows the array of the 96 microwells obtained after the photolithography process and chromium deposition. It can be seen from the picture that the actual dimensions obtained in the silicon wafers for the microwells were 40 $\mu$m on a side and with a pitch of 80 $\mu$m.

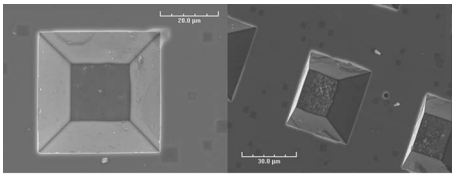

(a) (b)

**Fig. 3** SEM picture of a microwell: (a) top view of the microwell and (b) tilted view of the microwell obtained at a viewing angle of 30 deg.

Figure 3 shows two scanning electron micrographs (SEMs) of the microwells fabricated in the silicon substrate. A top view of a single microwell is shown in Fig. 3(a). It can be seen that the bottom of the microwell has a square shape with dimensions of about $20\times20$ $\mu$m. Figure 3(b) shows the SEM of one microwell after the sample holder was titled at an angle of 30 deg from the normal. The image was taken at a 1000× magnification.

### 2.2 *Heat Transfer Calculations*

As mentioned before, the purpose of the integration of a thermoelectric module in the *Centiwell* device is to condense water in the microwell array from ambient humidity. Thus, the thermoelectric module must be capable of removing heat at a rate required to reach the dew point temperature at the surface of the microwells. Heat transfer calculations were performed to estimate the operating temperature of the Peltier cooler and for obtaining the dew point temperature at the top of the substrate where the microwell array is located. Table 1 shows the dew point temperature calculated at 25°C for various humidity ratios. The humidity ratios considered in Table 1 are in accordance with the conditions at which the *Centiwell* device was tested. As a representative value, the heat transfer calculations were performed for an ambient temperature of 25°C.

In the thermal analysis, the only heat source for the silicon substrate was considered to be from natural convection of air on the top of the microwell array. A heat transfer

**Table 1** Dew point temperatures calculated at different relative humidity for an ambient temperature of 25°C.

| Relative humidity (%) | Dew point temperature (°C) |
|---|---|
| 25 | 3.25 |
| 30 | 6.1 |
| 35 | 8.3 |
| 40 | 10.2 |
| 45 | 12.1 |

coefficient of 10 $W/m^2K$ was assumed as a representative value for natural convection.[20] The contact resistance between the thermoelectric cooler and the back side of the substrate was neglected. To satisfy this condition, thermal grease (340 Silicone Heat Sink Compound, from Dow Corning Corporation) was used at the interface of the cooler and the substrate. In the heat transfer calculations, the thermal conductivity of silicon was 148 W/mK.[20] Newton's law of cooling was used [Eq. (1)] for the heat transfer calculations:

$$q'' = h(T_{\text{dew}} - T_{\infty}), \tag{1}$$

where $q''$ is the heat flux on the surface of the inkwell, $h$ is the convective heat transfer coefficient, $T$ is the temperature, subscript "*dew*" denotes dew point temperature, and subscript $\infty$ denotes the ambient temperature.

Phase change heat transfer due to condensation was neglected because it was estimated that the latent heat component from a thin film of the condensate was much lower compared to the convective component. To estimate the worst possible scenario, for an ambient temperature of 25°C and a relative humidity of 25%, the heat flux at the top surface of the silicon substrate was obtained as 217.5 $W/m^2K$

To maintain the top surface of the silicon substrate at the dew point temperature, all the heat gained by the substrate by convection must be dissipated or removed by the thermoelectric cooler. One dimensional form of the Fourier's law of conduction was used to estimate the temperature of the bottom surface of the wafer:

$$q'' = -k\frac{dT}{dy}, \tag{2}$$

where $k$ is the thermal conductivity of the silicon wafer, and $dT/dy$ is the temperature gradient in the silicon wafer.

Considering the distance between the bottom of the substrate and the bottom of the microwell as 490 $\mu$m, the temperature at the bottom of the substrate is obtained as 3.25°C. The temperature difference between the top and bottom surface of the silicon substrate is practically negligible due to the small thickness of the substrate ($\sim$500 $\mu$m). Therefore, the maximum cold side temperature of the thermoelectric module was determined to be 3.25°C (as mention before, the contact resistance was neglected).

Finally, the maximum power of the thermoelectric cooler was determined by performing a 1-D transient heat transfer analysis for the system. Typically, the maximum heat flux occurs at the initiation of the transient heat transfer process, because the temperature difference is maximum at this point. The transient analysis was performed by numerically solving Eq. (3) using a finite difference method:

$$\frac{1}{\alpha}\frac{\partial T}{\partial t} = \frac{\partial^2 T}{\partial y^2}, \tag{3}$$

where $\alpha$ is the thermal diffusivity (for silicon $\alpha = 90.7 \times 10^{-6}$ $m^2/s$),[21] and $dT/dt$ denotes the temporal gradient of the temperature.

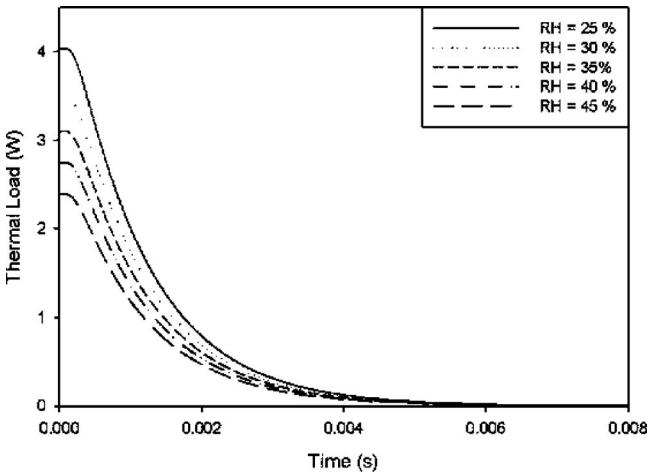


**Fig. 4** Thermal load variation with respect to time for different values of relative humidity.

Solving Eq. (3) numerically, the time needed to reach the steady state was calculated to be 10 ms. The cooling load with respect to time for different humidity conditions is shown in Figure 4. It can be seen from this figure that the maximum cooling load occurs at the beginning of the process, and it is higher for lower humidity ratios. This can be expected, since the dew point temperature required to achieve condensation of water droplets is higher for higher humidity.

Based on the thermal load (cooling) requirements estimated from the calculations described, the thermoelectric module TE-31-0.6-0.8 (manufactured by TE Technology, Incorporated) was chosen as a suitable Peltier cooler for the *Centiwell* microfluidic device. It can be observed from the plot in Fig. 4 that the maximum heat load to cool down the silicon substrate for a relative humidity of 25% is 4.036 W. The thermoelectric module TE-31-0.6-0.8 meets these dissipation requirements, since it is rated for a maximum cooling load of 4.8 W.

### 2.3 *Polyethylene Glycol Microbeads*

Polyethylene glycol (MW 20,000, Sigma-Aldrich) microspheres of 30 to 80 $\mu$m were obtained by filtering microspheres that were synthesized from molten PEG dispensed in a hot stir bath of mineral oil. The stirring speed was manipulated to obtain PEG microspheres (i.e., microbeads) of different size distributions.[22] The PEG microbeads were manually placed in the microwell array. As a proof of concept experiment, the PEG microbeads were not loaded with any biological materials. However, the PEG microbeads can be used to uniquely encapsulate biological materials (e.g., proteins, nucleic acids, or lipids) and placed in a definitive arrangement in the individual microwells of the *Centiwell* device. The PEG microbeads were manually placed into the microwells using a micromanipulator (Fig. 5).

In a commercial application such an operation can be automated using pneumatic robotic handlers specifically designed for picking and placing microbeads (e.g. SPBIOII Spotter by Mirai Bio, Hitachi Software, Waltham, MA). Another way to place the microbeads was achieved by de-

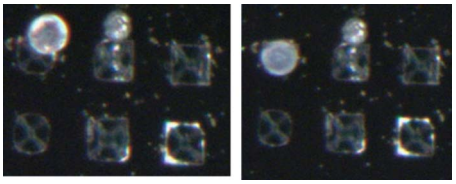

**Fig. 5** Images depicting the manual positioning of an individual PEG microbead into a microwell using a micromanipulator.

positing a number of PEG microbeads over the array of microwells. Using the edge of a filter paper, the microbeads were swept along the two directions of the microwell array, back and forth, several times to manipulate each microbead into a microwell. Subsequently, a final sweep was performed to remove excess PEG particles from the surface of the *Centiwell* substrate. With this technique, the microbeads of smaller size than the microwells were trapped into the microwells, and the excess microbeads were removed from the surface. Figure 1 shows the microwell array with PEG microbeads deposited in each microwell.

For better conceptualization, Fig. 6 shows an SEM picture of the empty microwells and microwells containing polystyrene microspheres of 25 $\mu$m diam (from Polysciences, Incorporated). The microbeads were placed inside the microwells only and the rest of the substrate was kept clean. This is especially important to avoid cross contamination when using different chemical species in different microwells.

## 3 Experimental Apparatus

The experiments for testing the *Centiwell* microfluidic device were conducted at the Center for Integrated Micromechanical Systems of Texas A&M University. The experimental apparatus is shown schematically in Fig. 7. The assembled *Centiwell* device was mounted on the stage of an atomic force microscope (AFM, Nanoscope IIIa from Digital Instruments). To improve the energy dissipation from the Peltier cooler to the AFM stage, thermal grease was applied at the interfaces of both top and bottom surfaces of the Peltier cooler.

Initially, the *Centiwell* microfluidic device was mounted on the AFM stage and contained PEG microbeads in every microwell. The AFM tip was positioned just above one of the microwells. The ambient humidity ratio during the experiments was recorded to be 30% with a corresponding dew point temperature of 6.2°C. The Peltier cooler was subsequently powered on (0.7 V, 0.28 A) to get the microwell surface cooled down to a temperature of 2°C. Once

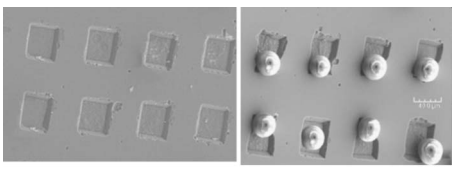

(a) (b)

**Fig. 6** SEM of a section of the array of microwells: (a) empty microwells and (b) individual polystyrene microbeads placed in each microwell.

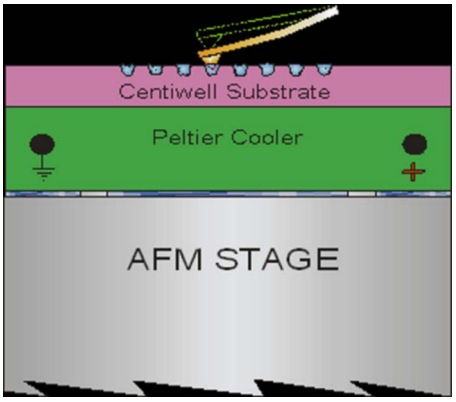


**Fig. 7** Schematic for "dipping" experiments conducted by mounting the *Centiwell* microfluidic device on an AFM stage.

the temperature of the silicon substrate reached below the dew point, condensed droplets of water were observed to form instantaneously on the surface of the *Centiwell* device (Fig. 7). After about 5 min, the power to the Peltier cooler was disconnected. It was observed that the condensed water droplets on the surface of the substrate evaporated immediately after the power to the Peltier cooler was disconnected. However, the water droplets trapped in the microwells were observed to dissolve the PEG microbeads and remain in the microwells when the power to the Peltier cooler was disconnected (Fig. 8).

Since PEG is hygroscopic, it spontaneously absorbs water from the ambient humidity. Due to this property, the PEG prevents (or minimizes) the evaporation of the condensed water in the solution. After the PEG solution ("ink") was obtained in the microwells, the AFM tip was lowered and dipped into the microwells containing the PEG "ink." This process is known as dipping, coating, or inking of the pen (scanning probe) for the subsequent DPN "writing" operation. The dipping of the AFM tip lasted about 2 min, after which the tip was raised by moving the stage vertically downward and the *Centiwell* device was dismounted from the stage of the AFM. The tips used in the experiments are nonconductive silicon-nitride-based scanning probes (model NP-20, with a top-60-nm-Au/bot-15-nm-Cr backside coating, Veeco Products, Santa Barbara, CA).

To prove the capability of the *Centiwell* device to deliver inks to different pens simultaneously, similar inking opera-

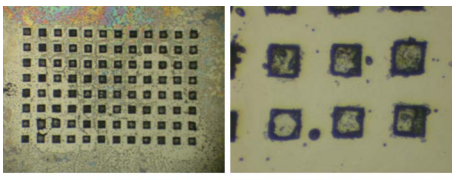

(a) (b)

**Fig. 8** Image showing the *Centiwell* substrate observed under a microscope after it is cooled below the dew point temperature. (a) The image shows condensed droplets of water in the microwells as well as on the top surface of the substrate. (b) Water droplets were trapped in the microwells after forming a PEG solution, while the condensed water droplets on the surface evaporated instantaneously after the power was disconnected.

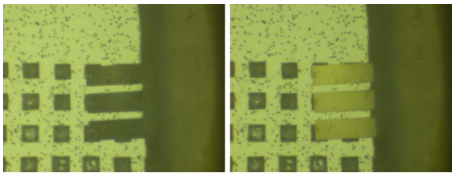

(a) (b)

**Fig. 9** Dipping process of a set of three DPN pens. (a) DPN pens close to the microwells before dipping, and (b) DPN pens dipped in the microwells and spontaneously pulled into the microwell by the capillary forces of the water meniscus.

tion was performed by dipping an array of pens into the microwells of the Centiwell. Figure 9 shows the dipping process of three pens of the A-18 Multiple-Pen Array (Manufactured by NanoInk Incorporated). A difference in the contrast of the light reflected from the back of the probes can be observed when the tip is dipped in the microwells [Fig. 9(b)] compared to just prior to dipping [Fig. 9(a)].

## 4 Results

When the inking process was concluded and the *Centiwell* device was dismounted, a mica substrate (PELCO® Mica Sheets, grade V5, from Ted Pella, Incorporated) was placed on the AFM stage and the DPN writing was carried out. This process was repeated several times to generate different patterns. A set of three lines of PEG were patterned by the DPN process using a single pen coated with PEG. The patterned lines were then imaged by lateral force microscopy (LFM), which is also known as "friction mode" and are shown in Fig. 10. After DPN patterning, the lines were scanned by LFM with the same PEG-coated tip at a scan rate of 6.7 Hz (tip velocity 407 $\mu$m/s). At such a high tip velocity, the scanning probe (pen) is not expected to deposit any ink on the substrate. The lines shown in Fig. 10 are 5 $\mu$m in length and were patterned at three different writing speeds of 5, 2, and 1 $\mu$m/s. The ambient relative humidity was registered to be 60% at the time of the DPN experiment. The thickness of the lines inversely varied with the writing speed.

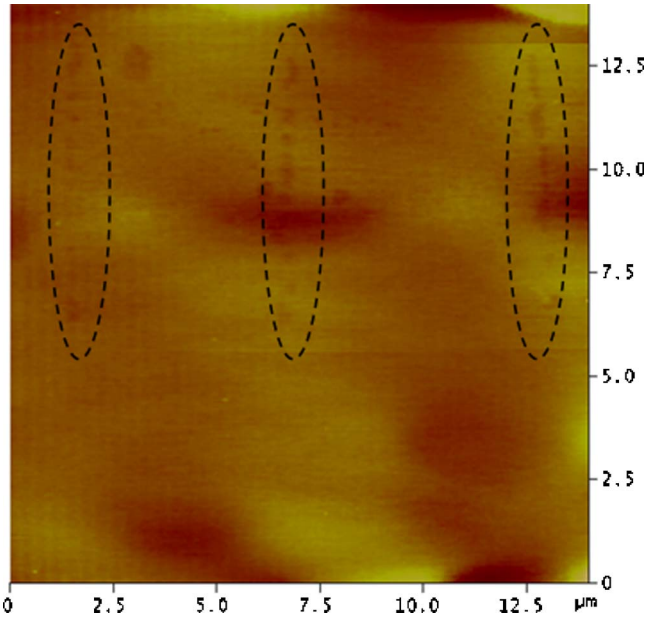


**Fig. 11** Discontinuous lines of PEG formed using the DPN process. The experiments were performed at an ambient humidity of 29%. The line widths are (left to right) 130, 235, and 285 nm, corresponding to writing speeds of 2, 1, and 0.5 $\mu$m/s. The patterned lines are highlighted by dotted lines that enclose the patterned lines.

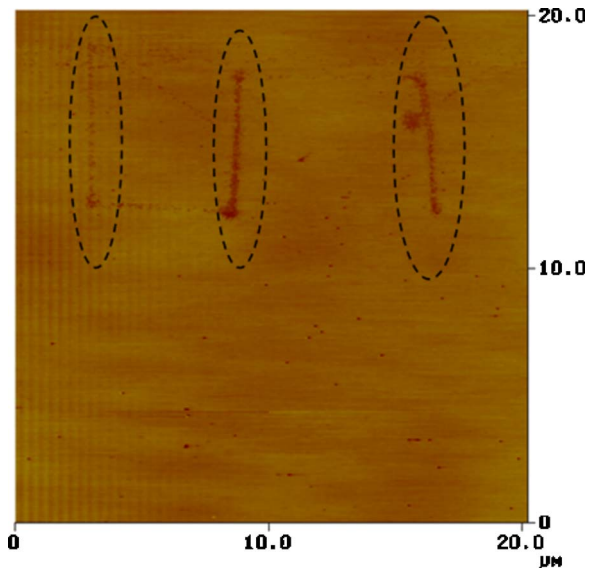


**Fig. 10** Lateral force microscopy image of a set of three lines patterned with PEG by DPN. Ambient humidity was recorded to be 60%. The line widths are (left to right) 285, 410, and 450 nm, corresponding to writing speeds of 5, 2, and 1 $\mu$m/s. The patterned lines are highlighted by dotted lines that enclose the patterned lines.

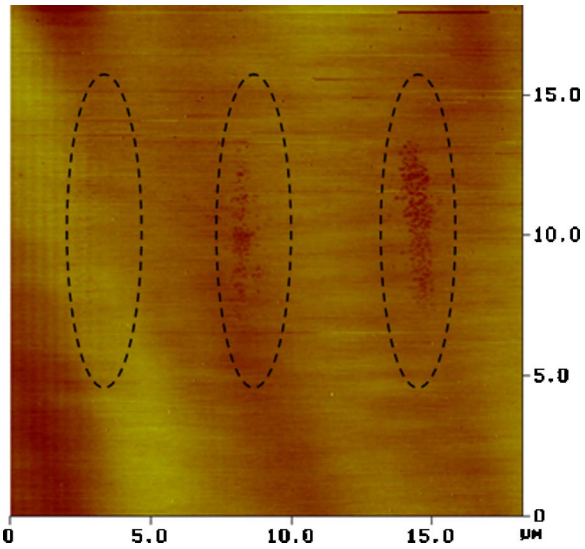


**Fig. 12** Discontinuous lines of PEG formed using the DPN process. LFM images show a set of three PEG lines patterned by DPN at an ambient humidity of 65%. The line widths are (left to right) ~150, 600, and 1120 nm, corresponding to writing speeds of 2, 1, and 0.5 $\mu$m/s. The patterned lines are highlighted by dotted lines that enclose the patterned lines.

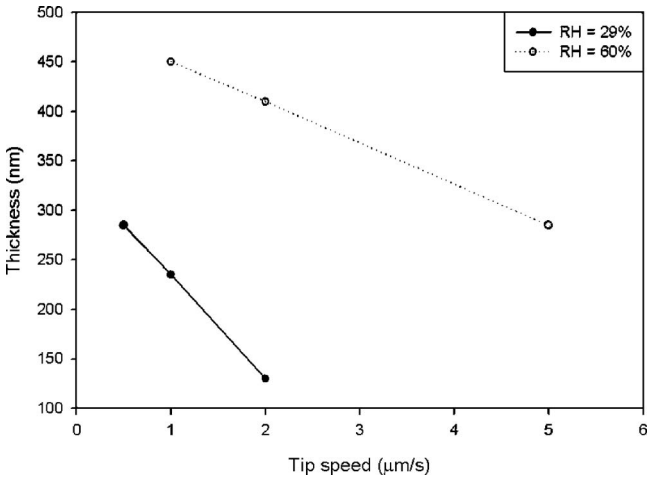


**Fig. 13** Variation of line width for nanopatterned features of PEG versus writing speed of the scanning probe tip under different relative humidity (RH).

A spot can be observed near the line on the extreme right in Fig. 10. This spot was formed at the end of the patterning (lithography) operation when the tip stayed in contact with the mica substrate, for about 45 s prior to disengaging the tip (pen). The spot was measured to be 800 nm in diameter. Traces of PEG materials were also observed along the trajectory of the tip while moving from one line to the next. The displacement of the tip from one line to the next was performed with the tip in contact with the mica substrate but at a relatively higher speed (20 $\mu$m/s).

Nanopatterning of a third set of three lines by DPN was performed for tip speeds of 2, 1, and 0.5 $\mu$m/s at an ambient humidity of 65 and 29%. Figures 11 and 12 show the image obtained by LFM for the set of three lines obtained with the PEG-coated tip at a scan rate of 6.7 Hz (tip velocity 407 $\mu$m/s). For these cases, the lines patterned at a writing speed of 2 $\mu$m/s is quite thin and is difficult to identify in the image. Although this line could not be measured properly, the section analysis of the images suggested that these lines are less than 150 nm in width.

It was found from the experiments that nanopatterning of PEG was strongly affected by the ambient humidity, producing larger width of the lines at higher values of relative humidity. The line width in the DPN process is known to depend on several factors, which include: temperature, ambient humidity, writing speed, surface roughness, ink surface diffusivity, and chemical affinity of the ink to the substrate.[1] The tip speed (writing speed) was also found to affect the line width in this study. In general, it was found that slower translation speeds of the AFM tip produced thicker lines. However, it was also observed that PEG patterns were difficult to obtain when the writing speed was lower than 0.5 $\mu$m/s.

A plot showing variation of line width for nanopatterned features of PEG versus writing speed is presented in Fig. 13 for different humidity ratios. The two curves from Fig. 13 show that for the nanopatterned lines, the width of the lines decreases as the tip speed increases. The graph also shows that for the same tip speed, the width of the nanopatterned lines increases with humidity. The graph shows that the absolute value of the slope of the graph decreases with increasing humidity.

Hence, it can be deduced from this trend that at high enough humidity values (say 90% or more), the line thickness will be insensitive to tip speed for a given range of tip speeds for PEG-based inks. The experimental apparatus used in this study had limited environmental control capabilities and was not capable of maintaining such high humidity values without preventing condensation of droplets on the instrument, hence nanopatterning at such high values of humidity could not be tested in this study.

Another set of experiments was performed using the DPN Multiple Pens. After the dipping operation of the three pens shown in Fig. 9, the *Centiwell* was removed from the AFM stage and a mica substrate was place instead for subsequent nanolithography.

Figure 14 shows a series of three LFM images corresponding to the diamond-like patterns of PEG generated by the three pens, respectively. The images were obtained individually at a scan rate of 6.7 Hz (tip velocity 407 $\mu$m/s) by directing the laser beam of the AFM to the corresponding pen for every pattern. Section analyses of the patterns

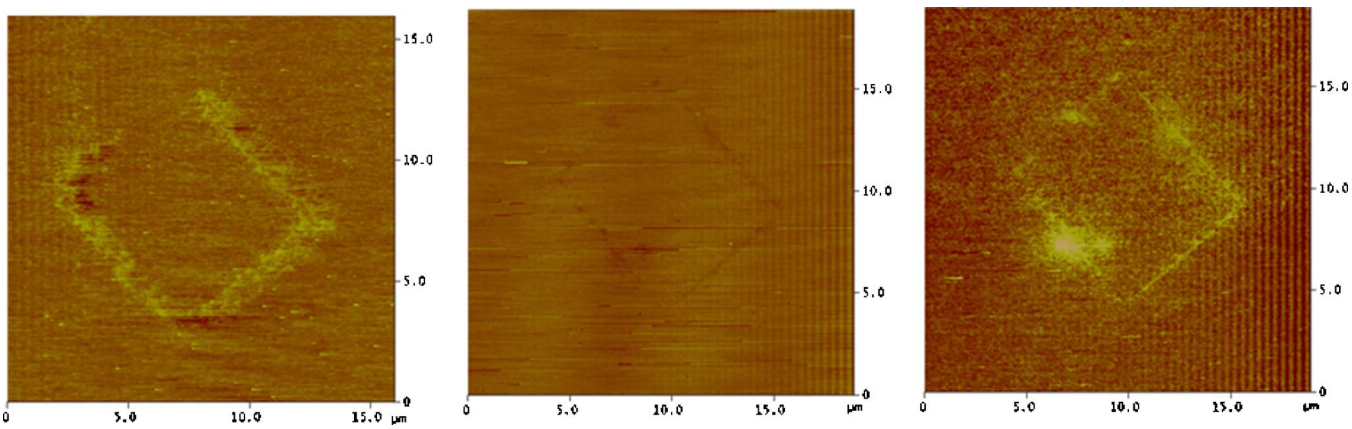


**Fig. 14** LFM images of a set of three PEG patterns obtained by parallel-write DPN at an ambient humidity of 70% and a writing speed of 0.8 $\mu$m/s. The line widths are (left to right) 1.3, 340, and ~520 nm.

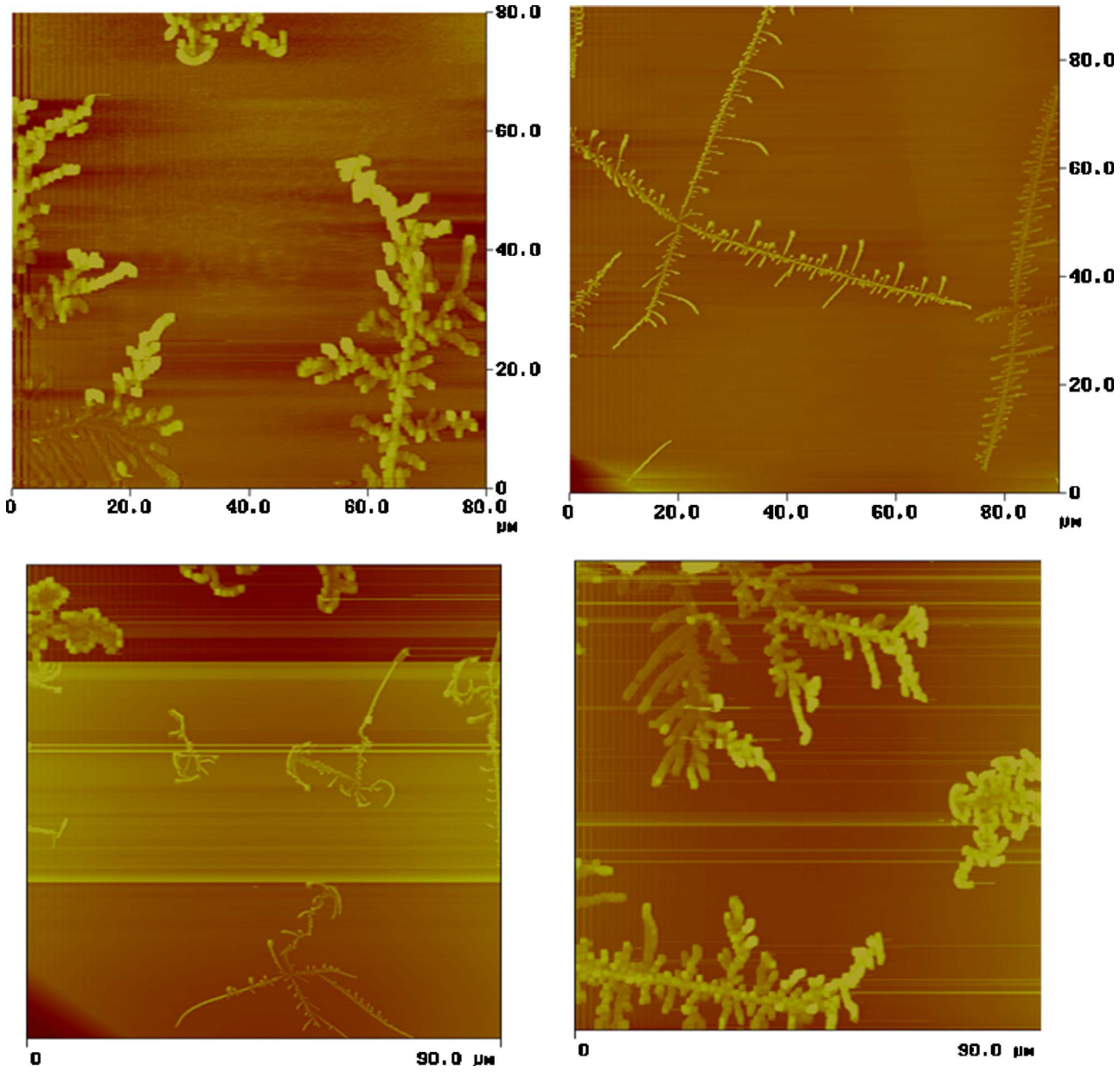


**Fig. 15** Images of fractal nanopatterns obtained by contacting a scanning probe (pen) coated with PEG ink on a mica substrate for 2 h. The images were obtained in contact mode (AFM) and the height of the fractal nanopatterns could be obtained in this study. The length of the fractal nanopatterns was observed to be 30 to 60 $\mu$m, with a width of 0.7 to 4.5 $\mu$m and height of 40 to 120 nm.

reveal line widths of (from left to right) of 1.3, 340, and 350 nm. The writing speed of the patterns was 0.8 $\mu$m/s in the three cases, and the ambient humidity at the time of the experiment was ~70%.

Finally, an interesting phenomenon was observed for DPN experiments involving large contact times and is reported here. After long contact times (~2 h) of the tip coated with PEG and in contact with the mica substrate, fractal patterns were obtained from LFM scans of the mica surface (Fig. 15). This is believed to occur by anomalous diffusion of PEG molecules on the substrate. Similar results have been reported for DPN operations of DDA (1-Dodecylamine) performed on mica for long contact times.[23] However, DPN patterns were observed only in friction mode (LFM) and the size of the fractal pattern was of the order of 1 to 2 $\mu$m. In the present work, several fractal patterns were observed in the friction mode (LFM) as well as in contact mode (AFM). Even in the contact mode (AFM), the fractal patterns were distinctly observed and lengths of the fractal features were found to be of the order of 30 to 60 $\mu$m with heights ranging from 40 to 120 nm. The areas containing the fractal patterns were scanned several times, and even after repeated scans, the shape of the patterns were not altered. This suggests that the fractal patterns of PEG formed a stable structure despite the weak binding affinity of PEG molecules to the mica surface. Figure 15 shows several fractal patterns obtained by DPN for large contact times.

## 5 Conclusions

The *Centiwell* microfluidic ink delivery device is designed, fabricated, assembled, and successfully tested in this study. This study proves the feasibility for using *Centiwell* microfluidic device as an ink delivery platform for maximizing the throughput of DPN to 96 different "inks" (or 96 unique chemical species). Volumes of about 1 pL per microwell are achieved, which can enable significant cost savings for nanolithography of expensive biological samples and reagents. Also, the *Centiwell* device has the capability to be expanded to a bigger array of microwells for handling larger numbers of inks (e.g., thousands of inks).

The *Centiwell* is successfully implemented for the intended purpose by delivering PEG solutions (formed in the microwells by condensing water droplets from ambient humidity) to the scanning probe tip, followed by successful nanolithography of the PEG ink. In general, it is found that widths of the nanopatterned lines increase as the humidity increases. The line widths are found to decrease as the tip speed increases.

The *Centiwell* demonstrates the proof-of-concept for a microfluidic architecture that can be expanded to handle multiple inks and to enable simultaneous nanopatterning of several hundreds of different inks. This platform provides the capability for exponential growth in ink-handling capacity. This approach mimics the exponential growth in device density of integrated circuits (ICs) that are responsible for the phenomenal growth of the microelectronics industry. It is envisioned that the utilization of a microfluidic platform such as *Centiwell* will serve as the stepping stone for similar progress in technological and commercial growth of nanosystems.

### *Acknowledgments*

The authors gratefully acknowledge the support for this study from the New Investigations Program (NIP 2005) of the Texas Space Grants Consortium (TSGC), Texas Engineering Experimentation Station (TEES), and the Mechanical Engineering Department faculty start-up grant that was awarded in January 2005.

### *References*

1. D. S. Ginger, H. Zhang, and C. A. Mirkin, "The evolution of dip-pen Nanolithography," *Angew. Chem., Int. Ed.* **43**(1), 30–45 (2004).
2. M. Zhang, D. Bullen, S. W. Chung, S. Hong, K. S. Ryu, Z. F. Fan, C. A. Mirkin, and C. Liu, "A MEMS nanoplotter with high-density parallel dip-pen nanolithography probe arrays," *Nanotechnology* **13**(2), 212–217 (2002).
3. X. Wang, K. S. Ryu, D. A. Bullen, J. Zou, H. Zhang, C. A. Mirkin, and C. Liu, "Scanning probe contact printing," *Langmuir* **19**(21), 8951–8955 (2003).
4. J. Zou, D. Bullen, X. F. Wang, C. Liu, and C. A. Mirkin, "Conductivity-based contact sensing for probe arrays in dip-pen nanolithography," *Appl. Phys. Lett.* **83**(3), 581–583 (2003).
5. P. Vettiger, M. Despont, U. Drechsler, U. Durig, W. Haberle, M. I. Lutwyche, H. E. Rothuizen, R. Stutz, R. Widmer, and G. K. Binnig, "Millipede—more than one thousand tips for future AFM data storage," *IBM J. Res. Dev.* **44**(3), 323–340 (2000).
6. W. P. King, T. W. Kenny, K. E. Goodson, G. L. W. Cross, M. Despont, U. T. Durig, H. Rothuizen, G. Binnig, and P. Vettiger, "Design of atomic force microscope cantilevers for combined thermomechanical writing and thermal reading in array operation," *J. Microelectromech. Syst.* **11**(6), 765–774 (2002).
7. E. M. Chow, G. G. Yaralioglu, C. F. Quate, and T. W. Kenny, "Characterization of a two-dimensional cantilever array with through-wafer electrical interconnects," *Appl. Phys. Lett.* **80**(4), 664–666 (2002).
8. T. Sulchek, R. J. Grow, G. G. Yaralioglu, S. C. Minne, C. F. Quate, S. R. Manalis, A. Kiraz, A. Aydine, and A. Atalar, "Parallel atomic force microscopy with optical interferometric detection," *Appl. Phys. Lett.* **78**(12), 1787–1789 (2001).
9. L. M. Demers and G. della Cioppa, "Nanotechnology to advance discovery R&D—Tutorial: dip pen nanolithography as a next-generation, massively parallel nanoarray platform," *Genet. Eng. News* **23**(15), 32–36 (2003).
10. A. D. Barone, J. E. Beecher, P. A. Bury, C. Chen, T. Doede, J. A. Fidanza, and G. H. McGall, "Photolithographic synthesis of high-density oligonucleotide probe arrays," *Nucleosides, Nucleotides Nucleic Acids* **20**(4-7), 525–531 (2001).
11. D. Banerjee, N. A. Amro, S. Disawal, and J. Fragala, "Optimizing microfluidic ink delivery for dip pen nanolithography," *J. Microlithogr., Microfabr., Microsyst.* **4**(2), 1-8, 023014–023021 (2005).
12. D. Banerjee et al., "Methods and apparatus for ink delivery to nanolithographic probe systems," U.S. Patent No. 7034854 (April 25 2006).
13. D. Banerjee, "Investigation of volume of fluids (VOF) method and system models for design of microfluidic ink delivery apparatus for dip pen nanolithography (DPN)," *Proc. Nanotechnol. NanoBio2005, Nano Sci. Technol. Institute (NSTI)*, pp. 680–683 (2005).
14. D. Banerjee, N. A. Amro, and J. Fragala, "Optimizing microfluidic ink delivery for dip pen nanolithography," *Proc. SPIE*, **5345**, 230–237 (2004).
15. D. Banerjee, J. Fragala, T. Duenas, R. Shile, and B. Rosner, "Planar capillary pumped ink delivery apparatus for dip pen nanolithography (DPN™)," *Proc. 7th Intl. Conf. Miniatur. Chem. Biochem. Anal. Syst. Micro Total Anal. Syst. (MicroTAS 2003)*, **57–60** (2003).
16. Inkwell™ Arrays Datasheet, see http://www.nanoink.net/docs/datasheets/datasheet_inkwell.pdf(Jul. 2006).
17. H. Seidel, L. Csepregi, A. Heuberger, and H. Baumgärtel, "Anisotropic etching of crystalline silicon in alkaline solutions. I. Orientation dependence and behavior of passivation layers," *J. Electrochem. Soc.* **137**(11), 3612–3626 (1990).
18. H. Seidel, L. Csepregi, A. Heuberger, and H. Baumgärtel, "Anisotropic etching of crystalline silicon in alkaline solutions. II. Influence of dopants," *J. Electrochem. Soc.* **137**(11), 3626–3632 (1990).
19. K. R. Williams, K. Gupta, and M. Wasilik, "Etch rates for micromachining processing—Part II," *J. Microelectromech. Syst.* **12**(6), 761–778 (2003).
20. F. P. Incropera and D. P. DeWitt, *Fundamentals of Heat and Mass Transfer*, 5th ed., p. 8, John Wiley, New York (2002).
21. A. F. Mills, *Basic Heat and Mass Transfer*, 2nd ed., Prentice Hall, Upper Saddler River, NJ (1999).
22. J. A. Rivas-Cardona, "Development of a microfluidic device for patterning multiple species by Scanning Probe Lithography," MS Thesis, Texas A&M Univ. (2006).
23. P. Manandhar, J. Jang, G. C. Schatz, M. A. Ratner, and S. Hong, "Anomalous surface diffusion in nanoscale direct deposition processes," *Phys. Rev. Lett.* **90**, 115505 (2003).

**Juan Alberto Rivas-Cardona** received his BS in mechanical engineering from the Universidad de Guanajuato, Mexico, and MS in mechanical engineering from Texas A&M University. He is a recipient of a graduate fellowship from ConaCyt (Mexico). Currently he is pursuing his PhD in mechanical engineering at Texas A&M University.

**Debjyoti Banerjee** received his PhD in mechanical engineering from the University of California, Los Angeles (with minor in MEMS) and received the "*2001 Best Journal Paper Award*" from the ASME Heat Transfer Division (HTD). He received three MS degrees and was invited to the membership of four national academic honor societies. He attended the Indian Institute of Technology, Kharagpur, for his bachelor of technology (honors). Since January 2005 he has been working as an assistant professor of mechanical engineering at Texas A&M University. His research interests are in thermo-fluidics (multiphase flow, boiling), microfluidics, MEMS, and nanotechnology (DPN, carbon nanotubes).